# Nanoparticles and nanocrystals of a new bidentate nickel(II) complex of N-[ethyl(propan-2-yl)carbamothioyl]-4-nitrobenzamide: synthesis, characterization, and crystal structures

Sohail Saeed [a], Naghmana Rashid [a], Rizwan Hussain [b], Jerry P. Jasinski [c], Amanda C. Keeley [c] & Sajid Khan [d]

[a] Department of Chemistry, Research Complex, Allama Iqbal Open University, Islamabad, Pakistan

[b] National Engineering & Scientific Commission, Islamabad, Pakistan

[c] Department of Chemistry, Keene State College, Keene, NH, USA

[d] School of Chemicals and Materials Engineering, National University of Science and Technology, Islamabad, Pakistan
Accepted author version posted online: 06 Nov 2012.Version of record first published: 18 Dec 2012.

PLEASE SCROLL DOWN FOR ARTICLE

# Nanoparticles and nanocrystals of a new bidentate nickel(II) complex of *N*-[ethyl(propan-2-yl)carbamothioyl]-4-nitrobenzamide: synthesis, characterization, and crystal structures

SOHAIL SAEED†*, NAGHMANA RASHID†, RIZWAN HUSSAIN‡, JERRY P. JASINSKI§, AMANDA C. KEELEY§ and SAJID KHAN¶

†Department of Chemistry, Research Complex, Allama Iqbal Open University, Islamabad, Pakistan
‡National Engineering & Scientific Commission, Islamabad, Pakistan
§Department of Chemistry, Keene State College, Keene, NH, USA
¶School of Chemicals and Materials Engineering, National University of Science and Technology, Islamabad, Pakistan

The nickel(II) complex of *N*-[ethyl(propan-2-yl)carbamothioyl]-4-nitrobenzamide has been synthesized and characterized by Fourier transform-infrared spectroscopy, elemental analysis, nuclear magnetic resonance spectroscopy, and mass spectrometry (atmospheric pressure chemical ionization mass spectrometry). The single-crystal X-ray structures of *N*-[ethyl(propan-2-yl)carbamothioyl]-4-nitrobenzamide (**1**) and *bis*[*N*-[ethyl(propan-2-yl)carbamothioyl]-4-nitrobenzamide]nickel(II) (**2**) have been determined from single-crystal X-ray diffraction data. Loss of the N–H proton resonance and the N–H stretching vibration and the shift of the $\nu_{C=O}$ and $\nu_{C=S}$ stretching vibrations confirm formation of the metal complex. These studies show that the metal complex is neutral in *cis*-configuration. The complex has been used as a single-source precursor for the deposition of nickel sulfide nanocrystals by thermolysis. The nickel sulfide nanocrystals were characterized by X-ray powder diffraction and transmission electron microscopy.

*Keywords*: Nickel complex; Crystal structure; *Cis*-configuration; Nanoparticles; Nanocrystals; p-XRD; TEM

## 1. Introduction

Design and self-assembly of metal coordination polymers has received attention [1–5] for crystallographic diversity and a myriad of applications [6, 7]. Although a variety of hybrid polymers have been synthesized with intriguing architectures and physical properties, it is still a challenge to prepare advanced conducting materials with predictable structures and properties through combination of ligands with metal ions. Judicious selection of ligands and suitable metal ions bearing the right coordination geometries is pivotal for designing metal complexes for the fabrication of nanostructured thin films and nanoparticles.

*Corresponding author. Email: sohail262001@yahoo.com

Thiourea chelating agents have been remarkable for analytical chemistry, especially for the trace analysis of metals in complex matrices. Coordination chemistry and potential applications of such ligands have only been explored to a small extent in the last few decades. With simultaneous presence of O, N, N', and S donors, substituted acylthiourea ligands exhibit various coordination modes: (a) O and S bonded to M (monobasic bidentate) [8], (b) only S bonded to M (neutral monodentate) [9], (c) O and N bonded to M (neutral bidentate) [10], and (d) O and S bonded to M and N is bonded to M' (monobasic bridging ligand) [11]. Substituted acylthiourea ligands, which do not form an intramolecular hydrogen bond, tend to coordinate predominately bidentate (S and O) to transition metal ions through sulfur and acyl oxygen [11]. Examples for this type of coordination are mononuclear complexes [ML$_2$], where M = Ni(II), Cu(II), Co(II), Zn(II), Cd(II), Pt(II), and Pd(II) and L = substituted acylthiourea derivatives [12]. Coordination solely through sulfur is rare and occurs only for complexes with Au(I) [13], Ag(I) [14], Hg(II) [15], and Cu(I) [16]. It has been suggested that intramolecular hydrogen bonding exists between the thiourea N–H moiety (where R/R'=H) and the amidic O-donor to form a six-membered ring, with the consequence that the ligands coordinate monodentate to metals through the sulfur donor [11].

There are relatively few reports on the deposition of nickel sulfide thin films from single-source precursors by chemical vapor deposition. The phase diagram of the Ni–S system is more complex than that of Fe or Co sulfides. In this system many crystalline phases and stoichiometries have been reported including the following: Ni$_{3+x}$S$_2$, Ni$_3$S$_2$, Ni$_{4+x}$S$_2$, Ni$_6$S$_5$, Ni$_7$S$_6$, Ni$_9$S$_8$, NiS, Ni$_3$S$_4$, and NiS$_2$ [17–19]. Some compounds, e.g. NiS and NiS$_2$, have been studied extensively, while for others only limited information is available. The NiS$_2$ (Vaesite) is a *p*-type semiconductor with a band gap of 0.5 eV [20], potentially useful in photo electrochemical solar cells [21, 22], IR detectors [23], catalysis [24], and sensors [25]. It is also used as a hydrodesulfurization catalyst and as a cathode material in rechargeable lithium batteries [26]. Nomura *et al*. studied the growth of NiS$_{1.03}$ from [Ni(S$_2$CNEt$_2$)$_2$] on silicon (1 1 1) substrates by low-pressure chemical vapor deposition (LP-CVD) [27]. Earlier, O'Brien *et al*. reported the deposition of nickel sulfide films from dithiocarbamate compounds of the type [Ni (S$_2$CNRR')$_2$], where RR' = Et$_2$, MeEt, Me$^n$Bu, or Me$^n$Hex, by AA [28] and LP-CVD methods [29] and also from xanthate compounds of the type [Ni(S$_2$COR)$_2$], where R = Et or $^i$Pr, by aerosol-assisted chemical vapor deposition (AACVD) [30]. Recently, Alam *et al*. used pyridine adducts of nickel(II) xanthates as single-source precursors for the deposition of nickel sulfide thin films by AACVD [31].

Our team has focused on the synthesis, characterization, crystal structures, biological activities, and material applications of new thiourea derivatives and their metal complexes [32–36]. In this communication, we have synthesized *N*-[ethyl(propan-2-yl)carbamothioyl]-4-nitrobenzamide (**1**) and *bis*[*N*-[ethyl(propan-2-yl)carbamothioyl]-4-nitrobenzamide]nickel (II) (**2**) and characterized each by spectroscopic techniques and crystal structures. In addition, the metal complex has been used as a single-source precursor for the deposition of nickel sulfide nanoparticles and nanocrystals by thermolysis.

## 2. Experimental

### 2.1. *Materials and reagents*

Analytical grade 4-nitrobenzoyl chloride (≥98.0%), ethyl isopropyl amine (99%), sodium thiocyanate (99%), nickel(II) acetate tetrahydrate (99%), and tetrabutylammonium bromide

(TBAB) (≥98%) were purchased from Sigma-Aldrich. Analytical grade solvents, such as tetrahydrofuran (THF), toluene, acetonitrile, n-hexane, dichloromethane, ethanol, methanol, chloroform, ethyl acetate, and others, were purchased from Sigma-Aldrich and Riedal-deHaen (Germany); ethanol and acetone were dried using standard procedures [37]. All manipulations were carried out in air except for thermolysis experiments. The synthesis of nickel sulfide nanoparticles and nanocrystals was carried out under $N_2$.

## 2.2. *Physical measurements*

Elemental analysis was performed by the University of Manchester micro-analytical laboratory. Infrared spectra were recorded on a Specac single-reflectance Attenuated Total Reflectance instrument (4000–400 cm$^{-1}$, resolution 4 cm$^{-1}$). Atmospheric pressure chemical ionization mass spectrometry of the ligand and nickel complex (MS-APCl) was recorded on a Micromass Platform II instrument. Metal analysis of the complex was carried out by Thermo iCap 6300 inductively coupled plasma optical emission spectroscopy. Melting points were recorded on a Barloworld SMP10 melting point apparatus. Thermal stability of the nickel complex was studied by thermogravimetry in an inert atmosphere, at a sample heating rate of 283 K min$^{-1}$, with a DuPont 2000 ATG. X-ray powder diffraction studies were performed on a Xpert diffractometer using Cu–Kα radiation. The samples were mounted flat and scanned between 20 and 65° with a step size of 0.05 with various count rates. The diffraction patterns were then compared to documented patterns in the International Center Diffraction Data (ICDD) index. Transmission electron microscopy (TEM) samples were prepared by evaporating a drop of a dilute suspension of the sample in n-hexane on a carbon-coated copper grid. Excess solvent was allowed to dry completely at room temperature. Transmission electron microscopic images were collected on a Philips CM200 transmission electron microscope using an accelerating voltage of 200 kV.

## 2.3. *Synthesis of the ligand and nickel complex*

### 2.3.1. Synthesis of *N*-[ethyl(propan-2-yl)carbamothioyl]-4-nitrobenzamide (1).

A solution of p-nitrobenzoyl chloride (0.01 mol) in anhydrous acetone (80 mL) and 3% TBAB in acetone was added dropwise to a suspension of sodium thiocyanate in acetone (50 mL) and the reaction mixture was refluxed for 45 min. After cooling to room temperature, a solution of ethyl isopropyl amine (0.01 mol) in acetone (25 mL) was added and the resulting mixture was refluxed for 2 h. The reaction mixture was poured into five times its volume of cold water, whereupon the thiourea precipitated. The solid product was washed with water and purified by re-crystallization from an ethanol–dichloromethane mixture (1 : 2) giving light yellow crystals. M.p.: 418–419 K. Yield: 2.7 g (76%). IR ($ν_{max}$/cm$^{-1}$): 3226 (NH), 2944, 2867 (C–H), 1671 (C=O), 1259 (C=S). $^1$H nuclear magnetic resonance (NMR) (400 MHz, CDCl$_3$) in δ (ppm): 8.40 (br s, 1H, CONH), 8.28 (d, 2H$_{meta}$, p-nitrophenyl), 8.01 (d, 2H$_{ortho}$, p-nitrophenyl), 4.03 (q, 2H, N–CH$_2$), 3.72 (m, H, N–CH), 1.38 (t, 3H,–CH$_3$), 1.29 (s, 6H, –CH$_3$); Anal. Calcd for C$_{13}$H$_{17}$N$_3$O$_3$S: C, 52.86; H, 5.80; N, 14.23; S, 10.86. Found: C, 52.84; H, 5.84; N, 14.21; S, 10.87. Mass (MS-APCI) (major fragment, *m/z*): 295[M+, C$_{13}$H$_{17}$N$_3$O$_3$S].

### 2.3.2. Synthesis of *bis*[*N*-[ethyl(propan-2-yl)carbamothioyl]-4-nitrobenzamide]nickel (II) (2).

A solution of nickel acetate (0.01 mol) in methanol (35 mL) was added dropwise

to a solution of the ligand in a 1 : 2 ratio with a small excess of ligand in ethanol (35 mL) at room temperature, and the resulting mixture was stirred for 3 h. The reaction mixture was filtered, washed with ethanol, and re-crystallized from a THF/acetonitrile mixture (1 : 1) giving yellowish golden crystals. M.p.: 431–432 K. Yield: 3.5 g (82%). IR ($\nu_{max}$/ cm$^{-1}$): 2927, 2853(Ar–H), 1508(C–O), 1533(C–N), 1142(C–S); Anal. Calcd for $C_{26}H_{32}N_6O_6S_2Ni$: C, 48.24; H, 4.98; N, 12.98; S, 9.91; Ni, 9.07. Found: C, 48.51; H, 4.95; N, 12.87; S, 9.94; Ni, 8.98. $^1H$ NMR (400 MHz, CDCl$_3$) in δ (ppm): 8.28 (d, 4H$_{meta}$, p-nitrophenyl), 8.01 (d, 4H$_{ortho}$, p-nitrophenyl), 4.05 (m, 4H, N–CH$_2$), 3.70 (m, 2H, N–CH), 1.35 (t, 6H, –CH$_3$), 1.28 (s, 12H, –CH$_3$); Mass (MS-APCI) (major fragment, *m/z*): 647[M+, $C_{26}H_{32}N_6O_6S_2Ni$].

### 2.4. *X-ray structure determination*

A crystal of **1** was mounted on a loop and placed in a 173 K compressed air stream on an Agilent Gemini-EOS single-crystal autodiffractometer at Keene State College (Keene, NH). Crystallographic data were collected using graphite monochromated 0.71073 Å Mo–Kα radiation and integrated and corrected for absorption using the *CrysAlisRed* (Oxford Diffraction, 2010 software package) [38]. The structures were solved using direct methods and refined using least-square methods on F$^2$ [39]. All non-hydrogen atoms were refined anisotropically. Hydrogens were included in calculated positions, assigned isotropic thermal parameters, and allowed to ride on their parent carbons. All other pertinent crystallographic details, such as h, k, l ranges, 2θ ranges, and R-factors, can be found in table 1.

### 2.5. *Synthesis of nickel sulfide nanoparticles/nanocrystals*

Nickel sulfide nanocrystals were prepared by pyrolyzing the nickel complex in oleylamine. In a typical reaction, 15 mL of oleylamine was refluxed under vacuum at 363 K for 45 min and then purged by nitrogen gas for 30 min, at same temperature. Precursor (0.3 g) was added into hot oleylamine and the reaction temperature was slowly increased to 443 or 503 K. The temperature was maintained for 1 h and the mixture was allowed to cool to room temperature. Addition of 30 mL methanol produced a black precipitate which was separated by centrifugation. The black residue was washed twice by methanol and dispersed in toluene or hexane for further characterizations.

## 3. Results and discussion

### 3.1. *Synthesis and spectroscopic characterization*

The thiourea derivative and its nickel complex were synthesized according to the reported procedure [40–45] with minor modifications as presented in Synthesis Scheme 1. The use of a phase transfer catalyst (PTC) as a method of agitating a heterogeneous reaction system is gaining recognition [46, 47]. In search of improving methods to prepare the target thiourea by reacting isothiocyanates with nucleophiles, we have found that the use of TBAB as PTC can produce isothiocyanates in good yield. The reaction proceeds via nucleophilic addition of the secondary amine to the isothiocyanate. We have conducted our reaction using TBAB as a PTC to synthesize the thiourea derivatives. Solid-state IR spectra of the thiourea

Table 1.   Crystal data and structure refinement for **1** and **2**.

|  | Compound **1** | Compound **2** |
|---|---|---|
| CCDC | 884,824 | 884,825 |
| Empirical formula | $C_{13}H_{17}N_3O_3S$ | $C_{26}H_{32}N_6O_6S_2Ni$ |
| Formula weight | 295.36 | 647.41 |
| Temperature | 173(2) K | 173(2) K |
| Wavelength | 1.54184 Å | 1.54184 Å |
| Crystal system | Triclinic | Orthorhombic |
| Space group | P−1 | F d d 2 |
| Unit-cell dimensions | $a = 7.5483(6)$ Å | $a = 24.8021(7)$ Å |
|  | $b = 13.2927(9)$ Å | $b = 16.5410(6)$ Å |
|  | $c = 15.2278(12)$ Å | $c = 14.3279(4)$ Å |
|  | $\beta = 96.700(6)°$ | $\beta = 90°$ |
| Volume | 1471.65(19) Å$^3$ | 5878.1(3) Å$^3$ |
| Z | 4 | 8 |
| Density (calculated) | 1.333 Mg m$^{-3}$ | 1.463 Mg m$^{-3}$ |
| Absorption coefficient | 2.060 mm$^{-1}$ | 2.711 mm$^{-1}$ |
| F(0 0 0) | 624 | 2704 |
| Crystal size | $0.34 \times 0.28 \times 0.08$ mm$^3$ | $0.44 \times 0.42 \times 0.22$ mm$^3$ |
| Theta range for data collection | 2.9918 to 71.4707° | 4.45 to 71.61° |
| Index ranges | $-9 <= h < 9, -16 < = k < 14, -18 < = l < = 18$ | $-30 < = h < = 30, -15 < = k < = 20, -17 < = l < = 17$ |
| Reflections collected | 9437 | 9538 |
| Independent reflections | 5581 [R(int) = 0.0422] | 2761 [R(int) = 0.0216] |
| Completeness to theta = 67.50° | 99.5% | 100.0% |
| Refinement method | Full-matrix least-squares on F$^2$ | Full-matrix least-squares on F$^2$ |
| Data/restraints/parameters | 5581/0/376 | 2761/1/200 |
| Goodness-of-fit on F$^2$ | 1.052 | 1.057 |
| Final R indices [I > 2sigma(I)] | R1 = 0.0651, wR2 = 0.1767 | R1 = 0.0355, wR2 = 0.0964 |
| R indices (all data) | R1 = 0.0738, wR2 = 0.1864 | R1 = 0.0368, wR2 = 0.0975 |
| Extinction coefficient | 0.0013(5) | 0.00(2) |
| Largest diff. peak and hole | 0.525 and −0.422 e.Å$^{-3}$ | 0.531 and −0.233 e.Å$^{-3}$ |

derivative and the metal complex at 4000–400 cm$^{-1}$ were compared and assigned by comparison [48]. N,N′-disubstituted thioureas behave both as monodentate and as bidentate ligands depending on the reaction conditions. Characteristic bands of N,N′-disubstituted thioureas are 3226 (NH), 2867, 2944 Ph (CH), 1671 (C=O), and 1259 (C=S), and there is a slight shift of C=O and C=S stretches due to coordination of the ligands to nickel.

Acylthioureas usually are bidentate to transition metal ions through the acyl oxygen and sulfur [49–51]. Fourier transform-infrared (FT-IR) spectra of the complex show significant changes compared with FT-IR spectra of the corresponding ligand. IR spectra of the complex show absorptions at $\upsilon_{max}$/cm$^{-1}$ 2853–2927 Ph (CH), 1508 (C–O), 1533 (C–N), and 1142 (C–S). The most striking changes are N–H stretches at 3226 cm$^{-1}$ in the free ligand, which disappears completely, in agreement with both ligand and complex structures. This indicates that the loss of proton comes from nitrogen of the (NH–CO) amide. Another striking change is observed with the carbonyl stretch. Vibration of carbonyl (1671 cm$^{-1}$) in the free ligand shifts to lower frequency upon complexation confirming that the ligand is coordinated to nickel(II) through oxygen and sulfur [52–56]. A comparative absorption pattern of the complex with the values of the free ligand demonstrates that coordination of a thiourea to nickel has a significant effect on $\upsilon$(NH), $\upsilon$(CO), and $\upsilon$(CS).
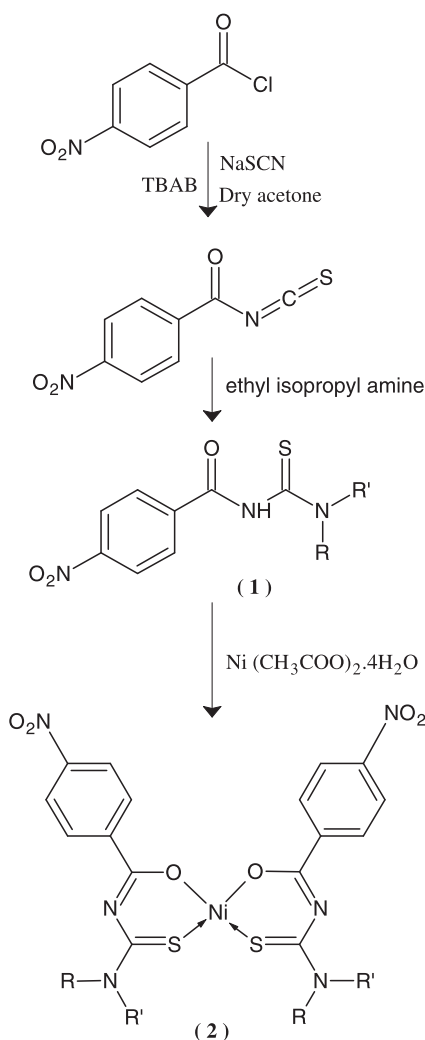
R = ethyl , R' = isopropyl

Scheme 1.  Preparation of **1** and **2**.

^{1}H NMR data for *N,N′*-disubstituted thiourea show that the NH resonates downfield. The proton chemical shifts are 8.40 for free NH and the aromatic protons appear downfield between 7.35 and 8.32 ppm. Coordinating or highly polar solvents like DMSO-d6 have profound effects on free NH proton chemical shifts and appear more downfield compared with $C_6D_6$, $CDCl_3$, and $CD_2Cl_2$. This shift can be attributed to hydrogen bonding between the NH and the sulfoxide (S=O). ^{1}H NMR data for the metal complex show aromatic protons at 8.28–8.01 ppm as reported earlier [57, 58]. Resonances due to NH of CONH in **1** completely disappear in **2**. This indicates that the loss of the proton was originally bonded to nitrogen of amide in the ligand and confirms the formation of the nickel complex. All characteristic chemical shifts were identified by their intensity and multiplicity patterns.
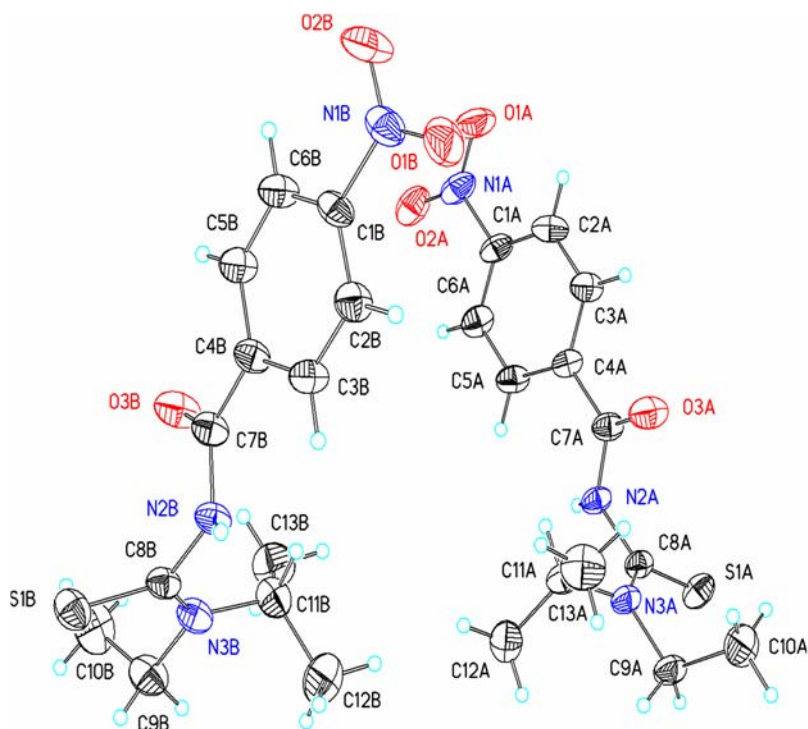
Figure 1. Perspective view of the two independent molecules in the asymmetric unit of **1** with atom-labeling scheme and 30% probability ellipsoids.
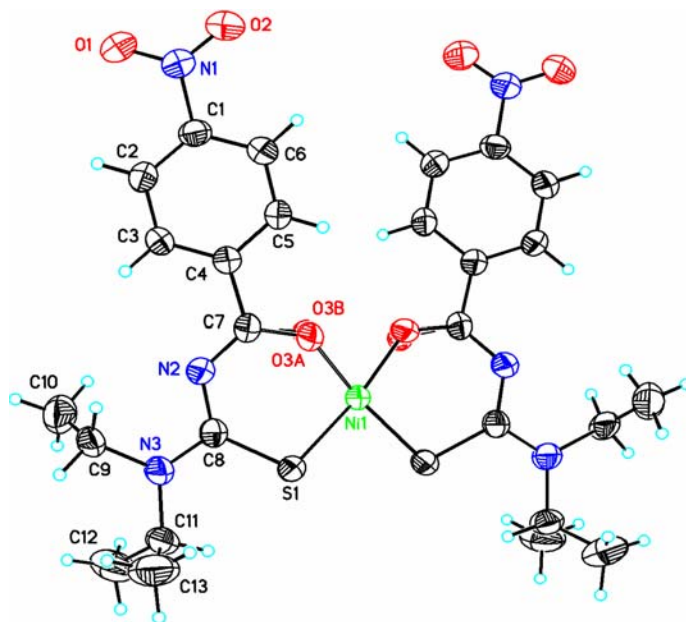


Figure 2. Perspective view of **2** which resides around a crystallographic inversion center on Ni1, and with atom-labeling scheme and 30% probability ellipsoids.

Table 2.   Selected bond lengths (Å) and angles (°) for **1** and **2**.

| Bond lengths (Å) | | | |
|---|---|---|---|
| Compound **1** | | Compound **2** | |
| S(1B)–C(8B) | 1.651(3) | Ni(1)–O(3A)#1 | 1.810(13) |
| O(1A)–N(1A) | 1.225(4) | Ni(1)–O(3A) | 1.810(14) |
| O(1B)–N(1B) | 1.224(3) | Ni(1)–O(3B) | 1.899(15) |
| O(2A)–N(1A) | 1.219(4) | Ni(1)–S(1) | 2.1429(8) |
| O(2B)–N(1B) | 1.231(4) | Ni(1)–S(1)#1 | 2.1430(8) |
| O(3A)–C(7A) | 1.212(3) | S(1)–C(8) | 1.757(3) |
| O(3B)–C(7B) | 1.217(3) | O(1)–N(1) | 1.208(4) |
| N(1A)–C(1A) | 1.483(4) | O(2)–N(1) | 1.210(4) |
| N(1B)–C(1B) | 1.474(3) | N(1)–C(1) | 1.481(4) |
| N(2A)–C(7A) | 1.367(3) | N(2)–C(7) | 1.302(4) |
| N(2A)–C(8A) | 1.427(3) | N(3)–C(9) | 1.490(4) |
| N(2A)–H(2NA) | 0.84(3) | C(1)–C(6) | 1.374(4) |
| N(2B)–C(7B) | 1.367(3) | C(3)–C(4) | 1.382(4) |
| N(2B)–C(8B) | 1.428(3) | C(3)–H(3) | 0.9300 |
| N(2B)–H(2NB) | 0.84(4) | O(1)–N(1)–C(1) | 118.5(3) |
| N(3A)–C(8A) | 1.331(4) | O(2)–N(1)–C(1) | 118.0(2) |
| N(3A)–C(9A) | 1.474(3) | C(7)–N(2)–C(8) | 123.3(2) |
| N(3A)–C(11A) | 1.481(4) | C(8)–N(3)–C(11) | 123.6(2) |
| N(3B)–C(8B) | 1.337(4) | C(8)–N(3)–C(9) | 119.1(3) |
| N(3B)–C(9B) | 1.470(4) | C(11)–N(3)–C(9) | 117.0(2) |
| N(3B)–C(11B) | 1.487(4) | C(6)–C(1)–C(2) | 122.5(3) |
| Bond angles (°) | | | |
| O(2A)–N(1A)–O(1A) | 124.4(3) | O(3A)#1–Ni(1)–O(3A) | 73.8(10) |
| O(2A)–N(1A)–C(1A) | 118.4(3) | O(3A)#1–Ni(1)–O(3B) | 80.3(17) |
| O(1A)–N(1A)–C(1A) | 117.1(3) | O(3A)–Ni(1)–O(3B) | 18.2(3) |
| O(1B)–N(1B)–O(2B) | 123.8(3) | O(3A)#1–Ni(1)–O(3B)#1 | 18.2(3) |
| O(1B)–N(1B)–C(1B) | 118.5(3) | O(3A)–Ni(1)–O(3B)#1 | 80.3(17) |
| O(2B)–N(1B)–C(1B) | 117.8(3) | O(3B)–Ni(1)–O(3B)#1 | 91(2) |
| C(7A)–N(2A)–C(8A) | 120.1(2) | O(3A)#1–Ni(1)–S(1) | 169.9(11) |
| C(7A)–N(2A)–H(2NA) | 119(2) | O(3A)#1–Ni(1)–S(1)#1 | 97.0(6) |
| C(8A)–N(2A)–H(2NA) | 116(2) | O(3A)–Ni(1)–S(1)#1 | 169.9(11) |
| C(7B)–N(2B)–C(8B) | 118.1(2) | S(1)–Ni(1)–S(1)#1 | 92.45(4) |
| C(7B)–N(2B)–H(2NB) | 120(2) | C(8)–S(1)–Ni(1) | 107.24(9) |
| C(8B)–N(2B)–H(2NB) | 113(2) | C(7)–O(3B)–Ni(1) | 128.6(17) |
| C(8A)–N(3A)–C(9A) | 119.1(2) | O(1)–N(1)–O(2) | 123.5(3) |
| C(8A)–N(3A)–C(11A) | 123.1(2) | H(10A)–C(10)–H(10C) | 109.5 |
| C(9A)–N(3A)–C(11A) | 117.5(2) | H(10B)–C(10)–H(10C) | 109.5 |
| C(8B)–N(3B)–C(9B) | 118.4(3) | C(13)–C(11)–N(3) | 109.3(3) |
| C(8B)–N(3B)–C(11B) | 123.9(2) | C(13)–C(11)–C(12) | 114.0(3) |
| C(9B)–N(3B)–C(11B) | 117.6(2) | N(3)–C(11)–C(12) | 111.5(3) |
| C(2A)–C(1A)–C(6A) | 122.9(3) | C(13)–C(11)–H(11) | 107.2 |
| C(2A)–C(1A)–N(1A) | 118.7(3) | N(3)–C(11)–H(11) | 107.2 |
| C(6A)–C(1A)–N(1A) | 118.4(3) | C(12)–C(11)–H(11) | 107.2 |
| C(6B)–C(1B)–C(2B) | 122.9(3) | C(11)–C(12)–H(12A) | 109.5 |

Table 3.   Weak intermolecular interactions for **1** [Å and °].

| D–H⋯A | d(D–H) | d(H⋯A) | d(D⋯A) | ∠(DHA) |
|---|---|---|---|---|
| N2A–H2NA⋯S1B#1 | 0.84(3) | 2.55(3) | 3.351(2) | 161(3) |
| N2B–H2NB⋯S1A#2 | 0.84(4) | 2.56(4) | 3.329(2) | 153(3) |
| C10A–H10A⋯S1B#3 | 0.96 | 2.85 | 3.727(4) | 153.1 |
| C11B–H11B⋯O2B#4 | 0.98 | 2.53 | 3.359(4) | 141.8 |

Notes: Symmetry transformations used to generate equivalent atoms: #1 x, y−1, z; #2 x, y+1, z; #3 x+1, y−1, z; and #4 −x+1, −y+1, −z+1.

### 3.2. *Single-crystal X-ray crystallography*

The molecular structures of *N*-[ethyl(propan-2-yl)carbamothioyl]-4-nitrobenzamide (**1**) and *bis*[*N*-[ethyl(propan-2-yl)carbamothioyl]-4-nitrobenzamide]nickel(II) (**2**) are shown in figures 1 and 2, respectively. Crystal data, refinement parameters, and selected bond lengths and angles are listed in tables 1 and 2, respectively. The structure of the nickel complex is in a *cis*-configuration with a slightly distorted square planar coordination of nickel by two oxygens and two sulfurs.

In **1**, there are two independent molecules in the asymmetric unit. Bond lengths are in normal ranges [59]. The mean plane of the nitro (C1A/N1A/O1A/O2A and C1B/N1B/O1B/O2B) is twisted by 2.4(4)° or 3.5(4)° with the mean plane of the benzene ring. The amide groups (C4A/C7A/O3A/N2A and C4B/C7B/O3B/N2B) and the thionyl groups (N1A/C8A/S1A/N3A and N1B/C8B/S1B/N3B) are twisted by 14.7(4)° or 12.5(1)° and 89.7(0)° or 87.4(5)° with the mean plane of the benzene ring, respectively. Crystal packing is stabilized by weak C–H…O intermolecular interactions (table 3, figure 3).
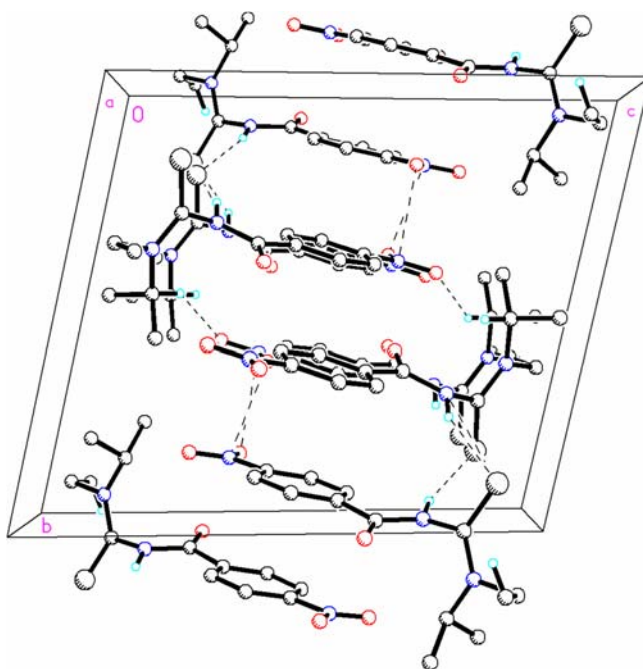


Figure 3.    Packing diagram of **1** viewed along the *a* axis. Dashed lines indicate weak N–H…S, C–H…S, and C–H…O intermolecular interactions. Remaining hydrogens have been removed for clarity.

Table 4.    Weak intermolecular interactions for **2** [Å and °].

| D–H…A | d(D–H) | d(H…A) | d(D…A) | (DHA) |
|---|---|---|---|---|
| C2–H2…O3B#1 | 0.93 | 2.51 | 3.34(3) | 149.1 |
| C5–H5…O1#2 | 0.93 | 2.49 | 3.284(4) | 143.7 |

Notes: Symmetry transformations used to generate equivalent atoms: #1 x + 1/4, −y + 5/4, z + 1/4 and #2 x − 1/4, −y + 5/4, z − 1/4.
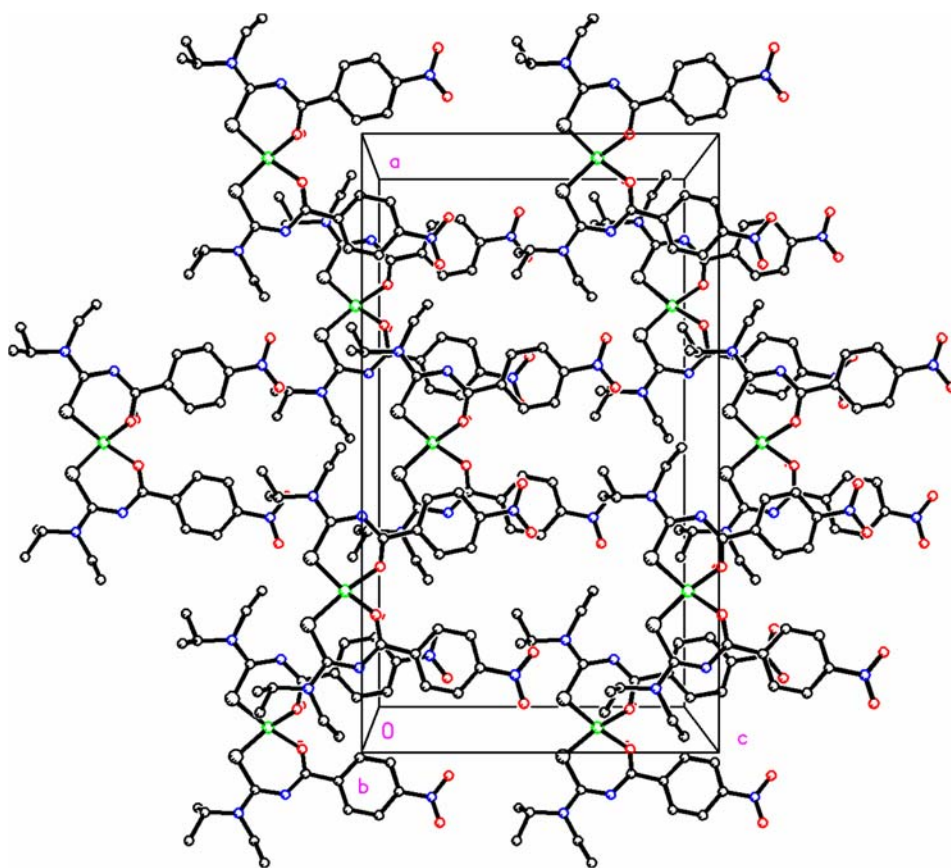
Figure 4.    Packing diagram of **2** viewed along the *a* axis. Hydrogens have been removed for clarity.

In **2**, the molecule resides around a crystallographic inversion center on nickel. Bond lengths are in normal ranges [59]. The oxygen in carbamothioyl is disordered over two sites with occupancies of 0.42(10) (O3A) and 0.58(10) (O3B). The six-membered car-bamothioyl groups (Ni1/O3A/C7/N2/C8/S1 and Ni1/O3B/C7/N2/C8/S1) adopt a slightly distorted boat or envelope conformation with puckering parameters Q, θ, and of 0.249(9) Å, 93(3)°, 236(3)° or 0.46(2) Å, 128(2)°, 170(3)°, respectively [60]. The mean plane of the nitro (C1/N1/O1/O2) is twisted by 5.4(4) Å with the mean plane of the benzene ring. The dihedral angle between the mean planes of the benzene rings is 16.0(9) Å. Crystal packing is stabilized by weak C–H...O intermolecular interactions (table 4, figure 4).

### 3.3. *Thermal decomposition studies and characterization of nickel sulfide nanoparticles and nanocrystals deposited from 2*

Thermal behavior of **2** has been examined by thermal gravimetric analysis (TGA) per-formed under an inert atmosphere of flowing nitrogen (20 mL/min) and a heating rate of 283 K/min. TGA of **2** shows two-step decomposition with rapid weight loss between 506 and 598 K and the second step between 601 and 848 K (table 5). The major part of the

Table 5.   Thermogravimetric analysis of **2**.

First-stage decomposition temperature range (K): 506–598
Second-stage decomposition temperature range (K): 601–848
Maximum degradation temperature range (K): 553–593
Weight loss at 1st stage decomposition (%): 62
Weight loss at 2nd stage decomposition (%): 16
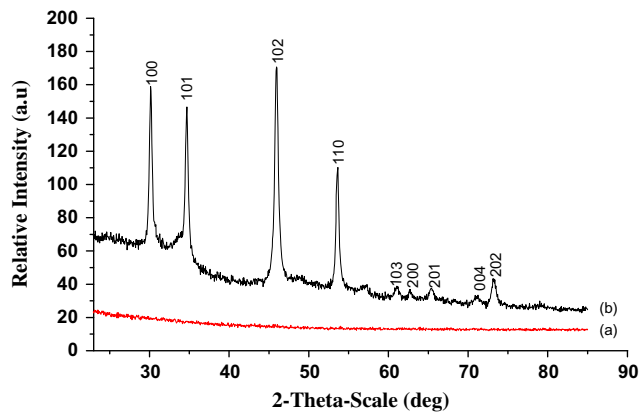Residual weight at 873 K (%): 18.63



Figure 5.   XRD pattern of NiS nanoparticles/nanocrystals prepared at (a) 443 K and (b) 503 K from precursor **2**.
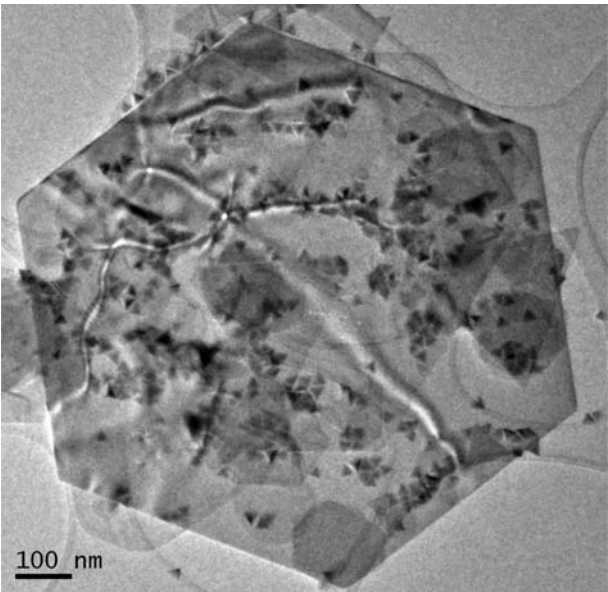


Figure 6.   TEM image of nickel sulfide nanoparticles and nanocrystals prepared from precursor **2** at 503 K.

complex degraded sharply at 553–593 K leaving residual amount of 18.63% which is close to the mass of NiS (calc. 19.04%). The XRD pattern for the NiS nanocrystals synthesized from **2** is shown in figure 5. The synthesis of the nickel sulfide nanoparticles and nanocrystals was carried out at 443 and 503 K. No deposition was obtained below 443 K. The material was almost in non-crystalline form at this low temperature. At 503 K, the XRD pattern of NiS nanocrystals shows diffraction patterns of hexagonal NiS and the space group P63/mmc with major diffraction peaks of (1 0 0), (1 0 1), (1 0 2), and (1 1 0) planes (ICDD: 00-002-1280). The TEM image (figure 6) showed the particles to be hexagonal and trigonal crystallites. A certain degree of agglomeration occurred, whereby the size of the nanoparticles could be approximated to 10–18 nm in length and nanocrystals to 1250 nm.

## 4. Conclusions

We have synthesized an unsymmetrical thiourea, *N*-[ethyl(propan-2-yl)carbamothioyl]-4-nitrobenzamide (**1**), and its nickel complex, *bis*[*N*-[ethyl(propan-2-yl)carbamothioyl]-4-nitrobenzamide] nickel(II) (**2**). The single-crystal X-ray structures of **1** and **2** have been determined. Complex **2** was used as a single-source precursor for the deposition of nickel sulfide nanoparticles (trigonal crystallites 10–18 nm in length) and nanocrystals (hexagonal crystallites 1250 nm in length).

### Supplementary crystallographic data

Crystallographic data for the structure reported in this article have been deposited with the Cambridge Crystallographic Data Center, CCDC 884,824 (**1**) and 884,825 (**2**). Copies of this information may be obtained free of charge from the Director, CCDC, 12 Union Road, Cambridge, CBZ IEZ, UK. Facsimile (44) 01223 336 033, E-mail: deposit@ccdc.cam.ac.uk or http://www.ccdc.cam.ac.uk/deposit.

### Acknowledgment

### References

[1] M. Kondo, M. Shimamura, S.I. Noro, S. Minakoshi, A. Asami, S. Kitagawa. *Chem. Mater.,* **12**, 1288 (2000).
[2] S. Banfi, L. Carlucci, E. Caruso, G. Ciani, D.M. Proserpio. *J. Chem. Soc., Dalton Trans.*, 2714 (2002).
[3] M. Antonietti. *Nature Mater.,* **2**, 9 (2003).
[4] G.F. Swiegers, T.J. Malefetse. *Chem. Rev.,* **100**, 3483 (2000).
[5] D.J. Hill, M.J. Mio, R.B. Prince, T.S. Hughes, J.S. Moore. *Chem. Rev.,* **101**, 3893 (2001).
[6] M. Eddaoudi, D.B. Moler, H. Li, B. Chen, T.M. Reineke, O.M. Yaghi. *Acc. Chem. Res.,* **34**, 319 (2001).
[7] L.R. MacGillivray, R.H. Groeneman, J.L. Atwood. *J. Am. Chem. Soc.,* **120**, 2676 (1998).
[8] R.A. Baily, K.L. Rothaupt. *Inorg. Chim. Acta,* **147**, 233 (1998).
[9] W. Bensch, M. Schuster. *Z. Anorg. Allg. Chem.,* **611**, 99 (1992).
[10] D.J. Che, G. Li, X.L. Yao, Q.J. Wu, W.L. Wang, Y. Zhu. *J. Organomet. Chem.,* **584**, 190 (1999).

[11] G. Kemp, A. Roodt, W. Purcell, K.R. Koch. *J. Chem. Soc., Dalton Trans.*, 4481 (1997).
[12] G. Binzet, N. Kulcu, U. Florke, H. Arslan. *J. Coord. Chem.,* **62**, 3454 (2009).
[13] A. Molter, F. Mohr. *Coord. Chem. Rev.,* **254**, 19 (2010).
[14] N. Gunasekaran, P. Ramesh, M.N.G. Ponnuswamy, R. Karvembu. *Dalton Trans.,* **40**, 12519 (2011).
[15] R. Richter, J. Sieter, I. Beyer, O. Lindqvist, L. Anderson. *Z. Anorg. Allg. Chem.,* **522**, 171 (1985).
[16] Y.F. Yuan, J.T. Wang, M.C. Gimeno, A. Laguna, P.G. Jones. *Inorg. Chim. Acta,* **324**, 309 (2001).
[17] G. Kullerud, R.A. Yund. *J. Petrol.,* **3**, 126 (1962).
[18] M.V. Swain. *J. Mater. Sci.,* **16**, 151 (1981).
[19] J.C. Barry, S. Ford. *J. Mater. Sci.,* **36**, 3721 (2001).
[20] S.D. Sartale, C.D. Lokhande. *Mater. Chem. Phys.,* **72**, 101 (2001).
[21] M. Sharon, G. Tamizhmani, C. Levy-Clement, J. Rioux. *Sol. Cells,* **26**, 303 (1989).
[22] Z. Zainal, N. Saravanan, H.L. Mien. *J. Mater. Sci. – Mater. Electron.,* **16**, 111 (2005).
[23] S. Leitz, G. Hodes, R. Tenne, J. Manassen. *Nature,* **326**, 863 (1987).
[24] S.T. Oyama. *J. Catal.,* **216**, 343 (2003).
[25] R.S. Mane, C.D. Lokhande. *Mater. Chem. Phys.,* **65**, 1 (2000).
[26] J. Cheon, D. Talaga, J.I. Zink. *Chem. Mater.,* **9**, 1208 (1997).
[27] R. Nomura, H. Hayata. *Trans. Mater. Res. Soc. Jpn,* **26**, 1283 (2001).
[28] P. O'Brien, J. Waters. *Chem. Vap. Deposition,* **12**, 620 (2006).
[29] P. O'Brien, J.H. Park, J. Waters. *Thin Solid Films,* **502**, 431 (2003).
[30] P.L. Musetha, N. Revaprasadu, M.A. Malik, P. O'Brien. *Mater. Res. Soc. Symp. Proc.,* **879E**, Z7.4 (2005).
[31] N. Alam, M.S. Hill, G. Kociok-Kohn, M. Zeller, M. Mazar, K.C. Molloy. *Chem. Mater.,* **20**, 6157 (2008).
[32] S. Saeed, N. Rashid, P.G. Jones, A. Tahir. *J. Heterocycl. Chem.,* **48**, 74 (2011).
[33] S. Saeed, N. Rashid, R. Hussain, P.G. Jones. *Eur. J. Chem.,* **2**, 77 (2011).
[34] S. Saeed, N. Rashid, P.G. Jones, M. Ali, R. Hussain. *Eur. J. Med. Chem.,* **45**, 1323 (2010).
[35] S. Saeed, N. Rashid, P.G. Jones, R. Hussain, M.H. Bhatti. *Cent. Eur. J. Chem.,* **8**, 550 (2010).
[36] S. Saeed, W.-T. Wong. *J. Heterocycl. Chem.,* **49**, 580 (2012).
[37] D.D. Perrin, W.L.F. Armarego, D.R. Perrin. *Purification of Laboratory Chemicals*, 3rd Edn, Pergamon Press, Oxford (1988)
[38] Oxford Diffraction. *CrysAlis PRO and CrysAlis RED*, Abingdon (2010).
[39] G.M. Sheldrick. *Acta Cryst.,* **A64**, 112 (2008).
[40] S. Saeed, N. Rashid, J.P. Jasinski, R.J. Butcher, R. Hussain. *Acta Cryst.,* **E66**, o2589 (2010).
[41] G.M.A. El-Reash, F.I. Taha, G. Badr. *Transition Met. Chem.,* **15**, 116 (1990).
[42] D.S. Mansuroglu, H. Arslan, U. Flörke, N. Kulcu. *J. Coord. Chem.,* **61**, 3134 (2008).
[43] Y.-M. Zhang, H.-X. Pang, C. Cao, T.-B. Wei. *J. Coord. Chem.,* **61**, 1663 (2008).
[44] H. Arslan, U. Flörke, N. Kulcu, M.F. Emen. *J. Coord. Chem.,* **59**, 223 (2006).
[45] G. Binzet, H. Arslan, U. Flörke, N. Kulcu, N. Duran. *J. Coord. Chem.,* **59**, 1395 (2006).
[46] K. Shao-Yong, X. Si-Jia. *ARKIVOC,* **x**, 63 (2006).
[47] T.B. Wei, J.C. Chen, X.C. Wang. *Synth. Commun.,* **26**, 1147 (1996).
[48] D. Fregona, L. Giovagnini, L. Ronconi, C. Marzano, A. Treevisan, B. Bordin. *J. Inorg. Biochem.,* **93**, 181 (2003).
[49] G.M.A. El-Reash, F.I. Taha, G. Badr. *Transition Met. Chem.,* **15**, 67 (1990).
[50] D.J. Che, X.L. Yao, G. Li, Y.H. Li. *J. Chem. Soc., Dalton Trans.*, 1853 (1998).
[51] V.R. Richter, L. Beyer, J. Kaiser. *Z. Anorg. Allg. Chem.,* **461**, 67 (1980).
[52] L. Beyer, E. Hoyer, L. Liebscher, H. Hartmann. *Z. Chem.,* **21**, 81 (1980).
[53] K.R. Koch, A. Irving, M. Matoetoe. *Inorg. Chim. Acta,* **206**, 193 (1993).
[54] K.R. Koch, C. Sacht, S. Bourne. *Inorg. Chim. Acta,* **232**, 109 (1995).
[55] M. Mikami, I. Nakagawa, T. Shimanouch. *Spectrochim. Acta,* **23A**, 1037 (1967).
[56] S. Saeed, N. Rashid, M. Ali, R. Hussain. *Eur. J. Chem.,* **1**, 200 (2010).
[57] K. Nakamoto. *Infrared and Raman Spectra of Inorganic and Coordination Compounds*, 4th Edn Edn, Wiley, New York, NY (1986)
[58] H. Arslan, N. Kulcu, U. Flörke. *Transition Met. Chem.,* **28**, 816 (2003).
[59] F.H. Allen, O. Kennard, D.G. Watson, L. Brammer, A.G. Orpen, R. Taylor. *J. Chem. Soc., Perkin Trans.,* **2**, S1–19 (1987).
[60] D. Cremer, J.A. Pople. *J. Am. Chem. Soc.,* **97**, 1354 (1975).